PL-TR--93-1010

PL-TR--
93-1010

CONSTANT-THRUST ORBIT-RAISING TRANSFER CHARTS

Salvatore Alfano
James D. Thorne

July 1993

Final Report

Approved for public release; distribution is unlimited.

PHILLIPS LABORATORY
Space and Missiles Technology Directorate
AIR FORCE MATERIEL COMMAND
KIRTLAND AIR FORCE BASE, NM 87117-5776

PL-TR--93-1010

This final report was prepared by the Phillips Laboratory, Kirtland Air Force Base, New Mexico, under Job Order 2181TA01. The project officer-in-charge was Lieutenant Colonel Salvatore Alfano (VTA).

This technical report has been reviewed and is approved for publication.

FOR THE COMMANDER

SALVATORE ALFANO
Lieutenant Colonel, USAF
Chief, Space and Missiles Dynamics Division

EUGENE R. DIONNE
Colonel, USAF
Director of Space and Missiles Technology

REPORT DOCUMENTATION PAGE

Form Approved
OMB No. 0704-0188

1. AGENCY USE ONLY *(Leave blank)*	2. REPORT DATE	3. REPORT TYPE AND DATES COVERED
	July 1993	Final Report; Aug 92 - May 93

4. TITLE AND SUBTITLE
CONSTANT-THRUST ORBIT-RAISING TRANSFER CHARTS

5. FUNDING NUMBERS
PE: 63401F
PR: 2181
TA: TA
WU: 01

6. AUTHOR(S)
Salvatore Alfano and James D. Thorne

7. PERFORMING ORGANIZATION NAME(S) AND ADDRESS(ES)
Phillips Laboratory
3550 Aberdeen Avenue, SE
Kirtland AFB, NM 87117-5776

8. PERFORMING ORGANIZATION REPORT NUMBER
PL-TR--93-1010

9. SPONSORING/MONITORING AGENCY NAME(S) AND ADDRESS(ES)

10. SPONSORING/MONITORING AGENCY REPORT NUMBER

11. SUPPLEMENTARY NOTES

12a. DISTRIBUTION/AVAILABILITY STATEMENT
Approved for public release; distribution is unlimited.

12b. DISTRIBUTION CODE

13. ABSTRACT *(Maximum 200 words)*

This report outlines a method to generate minimum-fuel trajectories between coplanar circular orbits for a vehicle with constant thrust. The rocket equation models the effects of continuous fuel expenditure while also serving to recast the solution in terms of accumulated velocity change. These orbit-raising solutions are globally mapped with no restrictions on initial thrust magnitude, intermediate eccentricity, or number of revolutions of the central body. Several examples are presented to verify the transfer charts and familiarize the reader with their use. These charts are useful tools for mission planners and satellite designers to assess preliminary fuel requirements for constant-thrust systems or to compare different propulsion technologies.

14. SUBJECT TERMS
Electric Propulsion, Thrust, Thruster, Efficiency, Orbits, Flight Maneuvers, Trajectories, Satellites (Artificial)

15. NUMBER OF PAGES
24

16. PRICE CODE

17. SECURITY CLASSIFICATION OF REPORT	18. SECURITY CLASSIFICATION OF THIS PAGE	19. SECURITY CLASSIFICATION OF ABSTRACT	20. LIMITATION OF ABSTRACT
Unclassified	Unclassified	Unclassified	

GENERAL INSTRUCTIONS FOR COMPLETING SF 298

The Report Documentation Page (RDP) is used in announcing and cataloging reports. It is important that this information be consistent with the rest of the report, particularly the cover and title page. Instructions for filling in each block of the form follow. It is important to ***stay within the lines*** to meet ***optical scanning requirements***.

Block 1. Agency Use Only *(Leave blank)*.

Block 2. Report Date. Full publication date including day, month, and year, if available (e.g. 1 Jan 88). Must cite at least the year.

Block 3. Type of Report and Dates Covered. State whether report is interim, final, etc. If applicable, enter inclusive report dates (e.g. 10 Jun 87 - 30 Jun 88).

Block 4. Title and Subtitle. A title is taken from the part of the report that provides the most meaningful and complete information. When a report is prepared in more than one volume, repeat the primary title, add volume number, and include subtitle for the specific volume. On classified documents enter the title classification in parentheses.

Block 5. Funding Numbers. To include contract and grant numbers; may include program element number(s), project number(s), task number(s), and work unit number(s). Use the following labels:

C	-	Contract	**PR**	-	Project
G	-	Grant	**TA**	-	Task
PE	-	Program Element	**WU**	-	Work Unit Accession No.

Block 6. Author(s). Name(s) of person(s) responsible for writing the report, performing the research, or credited with the content of the report. If editor or compiler, this should follow the name(s).

Block 7. Performing Organization Name(s) and Address(es). Self-explanatory.

Block 8. Performing Organization Report Number. Enter the unique alphanumeric report number(s) assigned by the organization performing the report.

Block 9. Sponsoring/Monitoring Agency Name(s) and Address(es). Self-explanatory.

Block 10. Sponsoring/Monitoring Agency Report Number. *(If known)*

Block 11. Supplementary Notes. Enter information not included elsewhere such as: Prepared in cooperation with...; Trans. of...; To be published in.... When a report is revised, include a statement whether the new report supersedes or supplements the older report.

Block 12a. Distribution/Availability Statement. Denotes public availability or limitations. Cite any availability to the public. Enter additional limitations or special markings in all capitals (e.g. NOFORN, REL, ITAR).

- **DOD** - See DoDD 5230.24, "Distribution Statements on Technical Documents."
- **DOE** - See authorities.
- **NASA** - See Handbook NHB 2200.2.
- **NTIS** - Leave blank.

Block 12b. Distribution Code.

- **DOD** - Leave blank.
- **DOE** - Enter DOE distribution categories from the Standard Distribution for Unclassified Scientific and Technical Reports.
- **NASA** - Leave blank.
- **NTIS** - Leave blank.

Block 13. Abstract. Include a brief *(Maximum 200 words)* factual summary of the most significant information contained in the report.

Block 14. Subject Terms. Keywords or phrases identifying major subjects in the report.

Block 15. Number of Pages. Enter the total number of pages.

Block 16. Price Code. Enter appropriate price code *(NTIS only)*.

Blocks 17. - 19. Security Classifications. Self-explanatory. Enter U.S. Security Classification in accordance with U.S. Security Regulations (i.e., UNCLASSIFIED). If form contains classified information, stamp classification on the top and bottom of the page.

Block 20. Limitation of Abstract. This block must be completed to assign a limitation to the abstract. Enter either UL (unlimited) or SAR (same as report). An entry in this block is necessary if the abstract is to be limited. If blank, the abstract is assumed to be unlimited.

INTRODUCTION

This report provides a simple tool for the orbital mission planner to use in designing optimal, coplanar, continuous-thrust trajectories. Six charts are presented that relate vehicle design parameters to orbit design parameters for circle-to-circle orbit raising.

Each transfer is accomplished with constant thrust through the entire flight path with no restriction on its magnitude. The direction of thrust is free to vary within the orbital plane with fuel expenditure modeled by the rocket equation. Intermediate eccentricity is allowed to grow and shrink for any number of orbit revolutions as optimally determined.

There has been a substantial amount of work done on low-thrust trajectories. Of particular relevance to this report are the works covering optimal, continuous, low-thrust transfers [Refs. 1 through 17]; included in these are numerous papers by Edelbaum [Refs. 3, 7, 8, and 11]. A mission planning tool for optimal, many-revolution, orbit transfers was presented by Wiesel and Alfano [Ref. 12] where an analytically derived solution was obtained and presented in graphical form.

The equations of motion used in this optimal control problem are in their complete form for the coplanar circle-to-circle case. The initial acceleration A_i appears in these equations and is allowed to vary from case to case as a parameter. Changing the spacecraft's initial acceleration always changes the minimum time to accomplish the orbit raising. To present the solution data in a user-friendly, universal form (Figs. 1 through 7), the problem is rescaled using the initial orbit radius and gravitational parameter of the central body; in addition, the time-of-flight t_f is replaced by the total accumulated velocity change Υ_f. The results of many such optimal cases are presented in graphical form, showing the relationship between spacecraft acceleration, propellant mass fraction, initial-to-final orbit radius ratio, and the minimum accumulated velocity change. The graphs themselves are composed of parametric families of optimal solutions assembled in comprehensive charts for interpolation by the orbital mission planner.

The charts cover the total range of spacecraft acceleration values. Many users of space assets are interested in minimum-time orbit raising and repositioning, so the high acceleration cases will be of increasing future interest as continuous-thrust propulsion technology improves.

EQUATIONS OF MOTION

The differential equations that define spacecraft motion are derived under the following assumptions:

- The force of thrust is constant and always in the plane of motion.
- The vehicle has a fixed propellant mass flow rate.
- The vehicle acceleration is due solely to the force of thrust and a spherically symmetric inverse square central gravitational field.

Using the defined nomenclature (page 13) and the above assumptions, the polar equations of motion are

$$\dot{r} = u \tag{1}$$

$$\dot{u} = \frac{v^2}{r} - \frac{\mu}{r^2} + \frac{A_i \sin\phi}{1 + \dot{m}\,t} \tag{2}$$

$$\dot{v} = -\frac{uv}{r} + \frac{A_i \cos\phi}{1 + \dot{m}\,t} \tag{3}$$

$$\dot{\theta} = \frac{v}{r} \tag{4}$$

where the dot denotes the first derivative with respect to time. The specific mass flow rate $\dot{m}$ is the actual mass flow rate divided by the initial mass. This value is negative when dealing with propellant loss.

OPTIMAL CONTROL FORMULATION

Given an initial and final radius, the fuel used between circular coplanar orbits must be minimized. This is equivalent to minimizing transfer time because $\dot{m}$ is assumed constant. From Bryson and Ho [Ref. 18], the Hamiltonian can be written as

$$H = 1 + \lambda_r \dot{r} + \lambda_u \dot{u} + \lambda_v \dot{v} \tag{5}$$

where the polar angle is omitted because the exact final position is not specified and θ does not appear in the equations of motion. The behavior of the Lagrange multipliers is given by

$$\dot{\lambda}_r = -\lambda_u \left(-\frac{v^2}{r^2} + \frac{2\mu}{r^3} \right) - \lambda_v \left(\frac{uv}{r^2} \right) \tag{6}$$

$$\dot{\lambda}_u = -\lambda_r + \lambda_v \left(\frac{v}{r} \right) \tag{7}$$

$$\dot{\lambda}_v = -\lambda_u \left(\frac{2v}{r} \right) + \lambda_v \left(\frac{u}{r} \right) \tag{8}$$

The partial of H with respect to the control parameter ϕ must equal zero

$$\frac{\partial H}{\partial \phi} = \left(\lambda_u \cos\phi - \lambda_v \sin\phi \right) \frac{A_i}{1 + \dot{m}t} = 0 \tag{9}$$

Knowing the acceleration term cannot be zero, the control law is established as

$$\tan\phi = \frac{-\lambda_u}{-\lambda_v} \tag{10}$$

The complete transfer is characterized by the initial choice of Lagrange multipliers. To date, the only closed-form solution that exists is for the many-revolution case where intermediate eccentricity is assumed to be zero and only tangential thrust is considered [Ref. 12]. Realizing that these multipliers can be scaled without affecting the control law or λ dynamics, λ_r is set to -1 and a numerical search is used to find the remaining two.

ACCUMULATED VELOCITY CHANGE

Accumulated velocity change, Υ, is defined here as the total velocity imparted by the force of thrust during the elapsed transfer time,

$$\Upsilon_f = \int_0^{t_f} \frac{A_i}{1 + \dot{m}t}\, dt \tag{11}$$

This formulation of the well-known rocket equation serves two purposes: it models the effect of fuel depletion and also defines the relationship between time and thrust-induced velocity change through the equation

$$\Upsilon_f = \frac{A_i}{\dot{m}} \ln(1+\dot{m}\, t_f) \tag{12}$$

Recasting the minimum-time solution in terms of Υ_f provides the means for a very compact graphical representation when considering the initial acceleration A_i and the propellant mass fraction,

$$m_p = -\dot{m}\, t_f \tag{13}$$

Given A_i, m_p, and Υ_f from a transfer chart, the specific mass flow rate and final time are computed as

$$\dot{m} = \frac{A_i}{\Upsilon_f} \ln(1 - m_p) \tag{14}$$

and

$$t_f = -\frac{m_p}{\dot{m}} \tag{15}$$

For the limiting case where $\dot{m}$ and m_p are zero, the total transfer time is simply

$$t_f = \frac{\Upsilon_f}{A_i} \tag{16}$$

CHART GENERATION AND DISCUSSION

Proper scaling can eliminate the dependence on a specific central attracting body and allow a global mapping of solutions. The following definitions for distance and time units are based on the initial radial distance r_i and the gravitational parameter of the central body μ:

$$1\ \mathrm{DU}^* = r_i \tag{17}$$

$$1\ \mathrm{TU}^* = \sqrt{\frac{r_i^3}{\mu}} \tag{18}$$

Although these definitions are dependent on the physical parameters of a given transfer, the equations of motion are not. Conveniently, the gravitational parameter is always 1 DU^{*3}/TU^{*2} and the initial values of the (r, u, v) array for any circle-to-circle coplanar transfer are simply ($1\,DU^*$, $0\,DU^*/TU^*$, $1\,DU^*/TU^*$). The final values are ($R\,DU^*$, $0\,DU^*/TU^*$, $\sqrt{1/R}\,DU^*/TU^*$) where R is the orbit ratio r_f/r_i. For this study only orbit raising is considered ($r_f > r_i$).

As previously mentioned, the initial Lagrange multiplier values completely define the transfer. To solve this two-point boundary value problem λ_r is set to -1 and a shooting method [Ref. 19] is used to find λ_u, λ_v, and t_f. Minimum-time solutions for a variety of orbit ratios and mass fractions are transformed to accumulated velocity change and plotted versus initial acceleration to produce Figures 1 through 7 (pages 14 through 20).

The ripples in the curves of Figures 1 through 4 reflect a transition region from gravitational force dominance to thrust dominance; they can be used to define the boundaries of low thrust (flat curve), intermediate thrust (rippled curve), and high thrust (constant upward sloping curve). Also, the ripples and subsequent upward slope testify to the additional cost of re-circularizing the final orbit. As seen in Figure 5, failure to complete a revolution during transfer increases the associated cost. The optimal steering law causes the eccentricity to increase for the first half of each revolution and then diminish in the latter half: the greater the thrust, the greater the eccentricity increase. If the desired radius is reached before completing a full revolution, the eccentricity must be zeroed out to meet the final condition of a circular orbit. The additional cost of this process is reflected by the peaks in the curves. When making more than five revolutions of the central body this effect is negligible because the induced eccentricity is very small and correctable with little additional maneuvering. If the final state is reached in less than one revolution, the intermediate eccentricity and associated cost grow with the shortness of the transfer arc. This is reflected in the positive slope of the curves. The cost of re-circularization diminishes as the ratio R increases because the gravitational force is less, making vehicle acceleration more effective. Also, when compared to Figure 1, the smaller ripples of Figures 2 through 4 reflect the increased thrust effectiveness due to mass loss.

Figure 6 characterizes all transfers where $A_i < 10^{-4}$ due to the constancy of accumulated velocity change for a given orbit ratio; this is in agreement with the results of Wiesel and Alfano [Ref. 12]. Figure 7 characterizes all transfers where $A_i > 4$ due to the constant slope of the $\mathcal{V}_f$ lines of Figures 1 through 4; the intercept value $\mathcal{V}_o$ is used to approximate the total accumulated velocity change through the empirical equation

$$\mathcal{V}_f = \mathcal{V}_o \sqrt{A_i} \tag{19}$$

CHART VERIFICATION AND USE

As a matter of convention, the input parameters will always be given as the array (r_i, r_f, μ, A_i, m_p). It is assumed the reader can determine total accumulated velocity to two significant figures from the transfer charts; six significant figures will be carried in all computations to reduce round-off error. Physical constants can be found in Reference 20. The data will be presented in the following form:

1) Unscaled Input Array
2) Scaled Input Array (Eqs. 17 and 18)
3) Accumulated velocity change from appropriate chart (Eq. 19, if needed)
4) Mass flow rate (Eq. 14, if needed)
5) Minimum time-of-flight (Eq. 15 or 16).

__Test Case #1__ The first test case is an Earth-Mars transfer where both planetary orbits are assumed to be circular and coplanar. The spacecraft starts in a heliocentric orbit free of Earth's gravitational field and finishes free of Mars' field. Earth escape and Mars capture are not considered.

1) (1.49598×10^{11} m, 2.27939×10^{11} m, 1.32712×10^{20} m^3/s^2, 8.33173×10^{-4} m/s^2, 0.0)
2) (1.0 DU*, 1.52368 DU*, 1.0 DU^{*3}/TU^{*2}, 0.1405 DU*/TU^{*2}, 0.0)
3) $\mathcal{V}_f = 0.50$ DU*/TU* (From Fig. 1)
4) $\dot{m} = 0$ /TU*
5) $t_f = 3.55872$ TU* = 1.78742×10^7 s.

The exact numerical answer is 3.53186 TU*, 1.77393×10^7 s, or 205.316 days.

__Test Case #2__ An Earth-Mars transfer solution can be found in Bryson and Ho [Ref. 18], but a mass flow rate of -12.9 lb/day is given for a 10^4 lb vehicle instead of the propellant mass fraction; interpolation will be needed to find a solution. The specific mass flow rate is -1.29×10^{-3} /day or -1.49306×10^{-7} /s; as a starting point m_p is set at 0.25.

1) (1.49598×10^{11} m, 2.27939×10^{11} m, 1.32712×10^{20} m^3/s^2, 8.33173×10^{-4} m/s^2, 0.25)

2) (1.0 DU*, 1.52368 DU*, 1.0 DU^{*3}/TU^{*2}, 0.1405 DU^*/TU^{*2}, 0.25)

3) $r_f = 0.54$ DU*/TU* (From Fig. 2)

4) $\dot{m} = -0.0748506$ /TU* $= -1.49026 \times 10^{-8}$ /s

5) $t_f =$ 3.33999 TU* $= 1.67756 \times 10^7$ s.

This final time solution is adequate because $\dot{m}$ from Equation 14 is within two significant figures of the original. For illustration purposes, m_p will be increased to 0.5 and interpolation will be used to refine the results and better determine the transfer time.

1) (1.49598×10^{11} m, 2.27939×10^{11} m, 1.32712×10^{20} m^3/s^2, 8.33173×10^{-4} m/s^2, 0.5)

2) (1.0 DU*, 1.52368 DU*, 1.0 DU^{*3}/TU^{*2}, 0.1405 DU^*/TU^{*2}, 0.5)

3) $r_f = 0.59$ DU*/TU* (From Fig. 3)

4) $\dot{m} = -0.165063$ /TU* $= -3.28637 \times 10^{-8}$ /s

5) $t_f =$ 3.02915 TU* $= 1.52144 \times 10^7$ s.

Linear interpolation of $\dot{m}$ produces a final time of 3.33951 TU*, 1.67729×10^7 s, or 194.131 days. This is within two significant figures of the Bryson and Ho solution of 193 days [Ref. 18] and the exact numerical solution of 192.748 days.

<u>Test Case #3</u> This case involves a LEO-GEO transfer using earth canonical units and metric units for a propellant mass fraction of 0.463, requiring interpolation between m_p values of 0.25 and 0.5.

1) (1.05 $DU_\oplus$, 6.61 $DU_\oplus$, 1.0 $DU_\oplus{}^3/TU_\oplus{}^2$, 4.0×10^{-3} m/s^2, 0.25)

2) (1.0 DU*, 6.29524 DU*, 1.0 DU^{*3}/TU^{*2}, 4.50079×10^{-4} DU^*/TU^{*2}, 0.25)

3) $r_f = 0.60$ DU*/TU* (From Fig. 2)

4) $\dot{m} = -2.15799 \times 10^{-4}$ /TU* $= -2.48596 \times 10^{-7}$ /s

5) $t_f =$ 1.25849×10^3 TU* $= 1.00565 \times 10^6$ s.

Increasing m_p to 0.5 yields

1) (1.05 $DU_\oplus$, 6.61 $DU_\oplus$, 1.0 $DU_\oplus{}^3/TU_\oplus{}^2$, 4.0×10^{-3} m/s^2, 0.5)

2) (1.0 DU*, 6.29524 DU*, 1.0 DU^{*3}/TU^{*2}, 4.50079×10^{-4} DU^*/TU^{*2}, 0.5)

3) $r_f = 0.60$ DU*/TU* (From Fig. 3)

4) $\dot{m} = -5.19952 \times 10^{-4}$ /TU* $= -5.98972 \times 10^{-7}$ /s

5) $t_f =$ 9.61628×10^2 TU* $= 8.34763 \times 10^5$ s.

Linear interpolation to match the given m_p produces a final time of 1.00556×10^3 TU*, 8.72902×10^5 s, or 10.103 days. This solution is close to the 10.0 day result of Prussing

[Ref. 17] and the exact numerical solution of 10.0808 days.

Test Case #4 This is a LEO-GEO transfer similar to #3 with the acceleration reduced by a factor of 1000 and a propellant mass fraction of 0.25.

1) $(1.05\,DU_{\oplus},\ 6.61\,DU_{\oplus},\ 1.0\,DU_{\oplus}{}^{3}/TU_{\oplus}{}^{2},\ 4.0\times10^{-6}\ m/s^{2},\ 0.25)$
2) $(1.0\,DU^{*},\ 6.29524\,DU^{*},\ 1.0\,DU^{*3}/TU^{*2},\ 4.50079\times10^{-7}\ DU^{*}/TU^{*2},\ 0.25)$
3) $\Upsilon_f = 0.60\,DU^{*}/TU^{*}$ (From Fig. 6)
4) $\dot{m} = -2.15799\times10^{-7}/TU^{*} = -2.48596\times10^{-10}/s$
5) $t_f = 1.25849\times10^{6}\ TU^{*} = 1.00565\times10^{9}$ s.

This case and the previous one involve low thrust (flat curve for Figures 1 through 4, Υ_f constant for a given orbit ratio R regardless of m_p or A_i). Scaling the acceleration causes an inverse scaling of transfer time. As expected, the final time is 1000 times greater than the test case #3 results for $m_p = 0.25$. This agrees with Reference 12.

Test Case #5 This is a high-thrust, LEO-GEO transfer; it is similar to #3 with the acceleration increased by a factor of 10^5 and a propellant mass fraction of 0.75.

1) $(1.05\,DU_{\oplus},\ 6.61\,DU_{\oplus},\ 1.0\,DU_{\oplus}{}^{3}/TU_{\oplus}{}^{2},\ 4.0\times10^{2}\,m/s^{2},\ 0.75)$
2) $(1.0\,DU^{*},\ 6.29524\,DU^{*},\ 1.0\,DU^{*3}/TU^{*2},\ 45.0079\,DU^{*}/TU^{*2},\ 0.75)$
3) $\Upsilon_o = 6.4\,DU^{*}/TU^{*}$ (From Fig. 7), $\Upsilon_f = 42.9363\,DU^{*}/TU^{*}$ (Eq. 19)
4) $\dot{m} = -1.45309/TU^{*} = -1.67292\times10^{-3}/s$
5) $t_f = 0.516144\,TU^{*} = 448.05\,s$.

The exact numerical solution is 445.582 s.

Test Case #6 The last test case is an intermediate-thrust, Earth-Jupiter transfer where both planetary orbits are assumed to be circular and coplanar. Earth escape and Jupiter capture are not considered.

1) $(1.49598\times10^{11}\,m,\ 7.78299\times10^{11}\,m,\ 1.32712\times10^{20}\,m^{3}/s^{2},\ 1.77902\times10^{-4}\,m/s^{2},\ 0.75)$
2) $(1.0\,DU^{*},\ 5.20260\,DU^{*},\ 1.0\,DU^{*3}/TU^{*2},\ 0.03\,DU^{*}/TU^{*2},\ 0.75)$
3) $\Upsilon_f = 1.1\,DU^{*}/TU^{*}$ (From Fig. 4)
4) $\dot{m} = -0.037808/TU^{*} = -1.89897\times10^{5}\ /s$
5) $t_f = 19.8371\,TU^{*} = 9.96348\times10^{7}\,s = 1153.18$ days.

The exact numerical solution is 1150.34 days.

CLOSING REMARKS

This report outlines a method to generate minimum-fuel circle-to-circle coplanar transfer trajectories for a vehicle with constant thrust. Accumulated velocity change replaces the time-of-flight while also accounting for propellant mass loss. The solutions are globally mapped with no restrictions on initial thrust magnitude, intermediate eccentricity, or number of revolutions of the central body. Several examples are presented that verify the transfer charts and show their ease of use. These charts are useful tools for mission planners and satellite builders to assess preliminary fuel requirements or to compare different propulsion technologies.

REFERENCES

1. Levin, E., Low-Thrust Transfer Between Circular Orbits, ASME Paper No. 59-AV-2, 1959.

2. Faulders, C.R., "Optimum Thrust Programming of Electrically Powered Rocket Vehicles in a Gravitational Field," American Rocket Society Journal, pp. 954-960, October 1960.

3. Edelbaum, Theodore N., "Propulsion Requirements for Controllable Satellites," ARS Journal, Vol. 31, pp. 1079-1089, August 1961.

4. Melbourne, William G., "Three-Dimensional Optimum Thrust Trajectories for Power Limited Propulsion Systems," ARS Journal, pp. 1723-1728, December 1961.

5. Lindorfer, W., and Moyer, H.G., "Application of a Low Thrust Trajectory Optimization Scheme to Planar Earth-Mars Transfer," ARS Journal, pp. 260-262, February 1962.

6. Faulders, C.R., "Optimum Thrust Programming of Electrically Powered Rocket Vehicles for Earth Escape," AIAA Journal, Vol. 1, No. 1, pp. 233-234, January 1963.

7. Edelbaum, Theodore N., "Optimum Low-Thrust Rendezvous and Station Keeping," AIAA Journal, pp. 1196-1201, July 1964.

8. Edelbaum, Theodore N., "Optimum Power-Limited Orbit Transfer in Strong Gravity Fields," AIAA Journal, Vol. 3, No. 5, pp. 921-925, May 1965.

9. Shi, Yun Y., and Eckstein, M.C., "Ascent or Descent from Satellite Orbit by Low Thrust," AIAA Journal, Vol. 4, pp. 2203-2209, December 1966.

10. Eckstein, Martin C., and Shi, Y.Y., "Low Thrust Elliptical Spiral Trajectories of a Satellite with Variable Mass," AIAA Journal, Vol. 5, pp. 1491-1494, August 1967.

11. Edelbaum, Theodore N., Sackett, Lester L., and Malchow, Harvey L., Optimal Low Thrust Geocentric Transfer, Paper No. 73-1074, AIAA 10th Electric Propulsion Conference, Lake Tahoe, Nevada, October-November 1973.

12. Wiesel, William E., and Alfano, Salvatore, "Optimal Many-Revolution Orbit Transfer," Journal of Guidance, Vol. 8, No. 1, pp. 155-157, January-February 1985.

13. Kechichian, Jean A., Low Thrust Eccentricity Constrained Orbit Raising, Paper No. AAS 91-156, AAS/AIAA Spaceflight Mechanics Meeting, Houston, Texas, February 1991.

14. Broucke, Roger A., Low-Thrust Trajectory Optimization in an Inverse Square Force Field, Paper No. AAS 91-159, AAS/AIAA Spaceflight Mechanics Meeting, Houston, Texas, February 1991.

15. Bauer, Timothy A., Near-Optimum Low-Thrust Transfer in Semi-Major Axis and Eccentricity, Paper No. AAS 92-134, AAS/AIAA Spaceflight Mechanics Meeting, Colorado Springs, Colorado, February 1992.

16. Burton, Rodney L., and Wassgren, Carl, "Time-Critical Low-Thrust Orbit Transfer Optimization," Journal of Spacecraft and Rockets, Vol. 29, No. 2, pp. 286-288, March-April 1992.

17. Prussing, John E., Equation for Optimal Power-Limited Spacecraft Trajectories, Paper No. AAS 93-147, AAS/AIAA Spaceflight Mechanics Meeting, Pasadena, California, February 1993.

18. Bryson, Arthur E., and Ho, Y., Applied Optimal Control, pp. 42-89, Hemisphere Publishing Corporation, Washington, D.C., 1975.

19. Press, William H., Teukolsky, S.A., Vetterling, W.T., and Flannery, B.P., Numerical Recipes in Fortran, pp. 749-751, Cambridge University Press, Cambridge, 1992.

20. *Explanatory Supplement to the Astronomical Almanac*, Seidelmann, P. K. (Ed), pp. 696,704, University Science Books, Mill Valley, California, 1992.

NOMENCLATURE

A_i = initial vehicle acceleration
DU^* = scaled distance unit
$DU_\oplus$ = earth distance unit
H = Hamiltonian
m = meters
$\dot{m}$ = specific propellant mass flow rate of vehicle
m_p = propellant mass fraction
r = radial distance of vehicle from attracting center
r_f = final radial distance
r_i = initial radial distance
R = ratio of final to initial radial distance
s = seconds
t = time
t_f = total time of transfer (time-of-flight)
TU^* = scaled time unit
$TU_\oplus$ = earth time unit
u = radial component of velocity
u = radial component of velocity
v = transverse component of velocity
Υ_f = total accumulated velocity change
Υ_o = accumulated velocity change intercept value
θ = polar angle
λ = Lagrange multiplier
λ_r = Lagrange multiplier associated with r
λ_u = Lagrange multiplier associated with u
λ_v = Lagrange multiplier associated with v
μ = gravitational constant of attracting center
ϕ = in-plane thrust direction angle (control parameter)

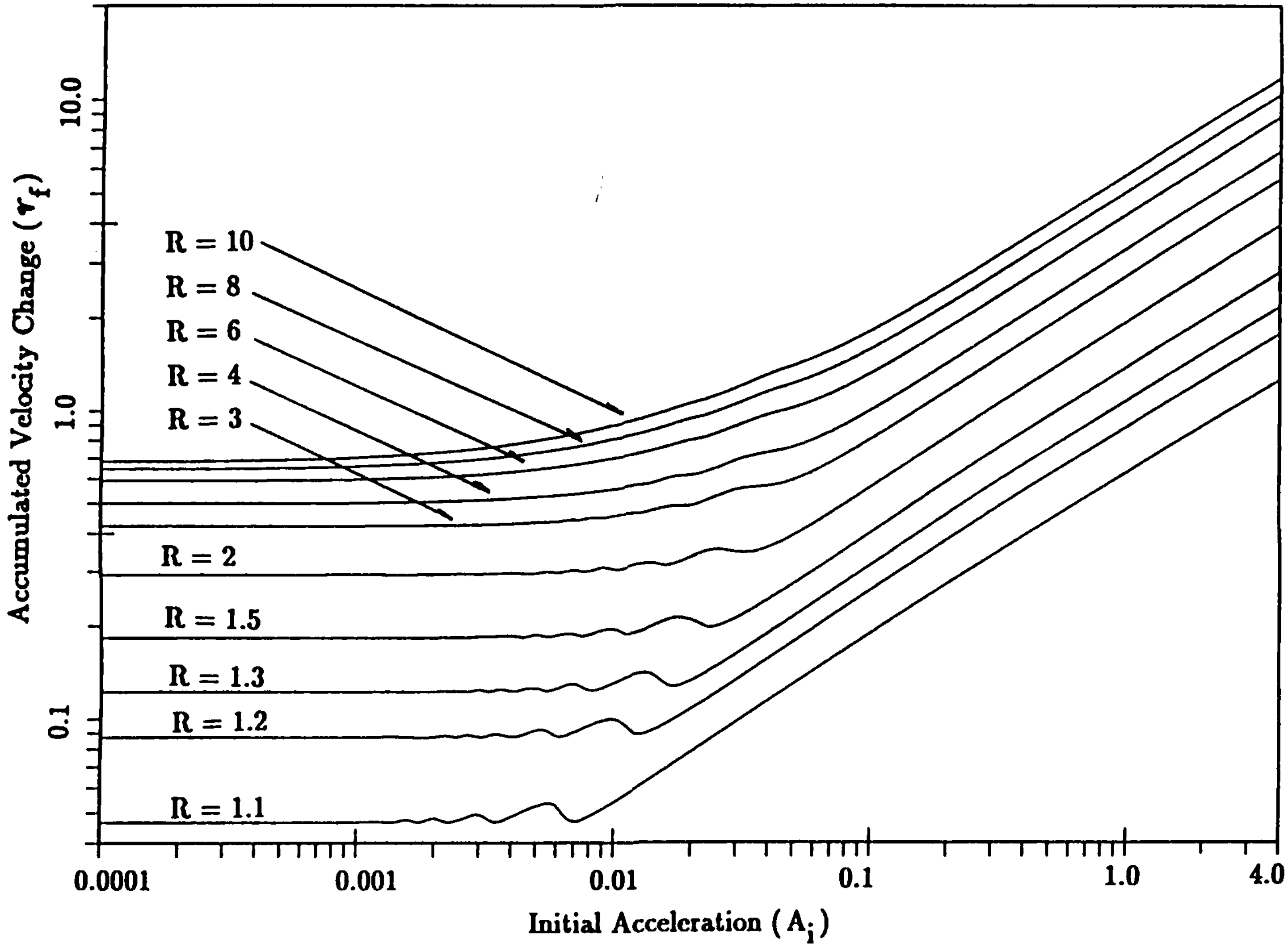

FIG. 1 Υ_f contours for various orbit ratios R ($m_p = 0$)

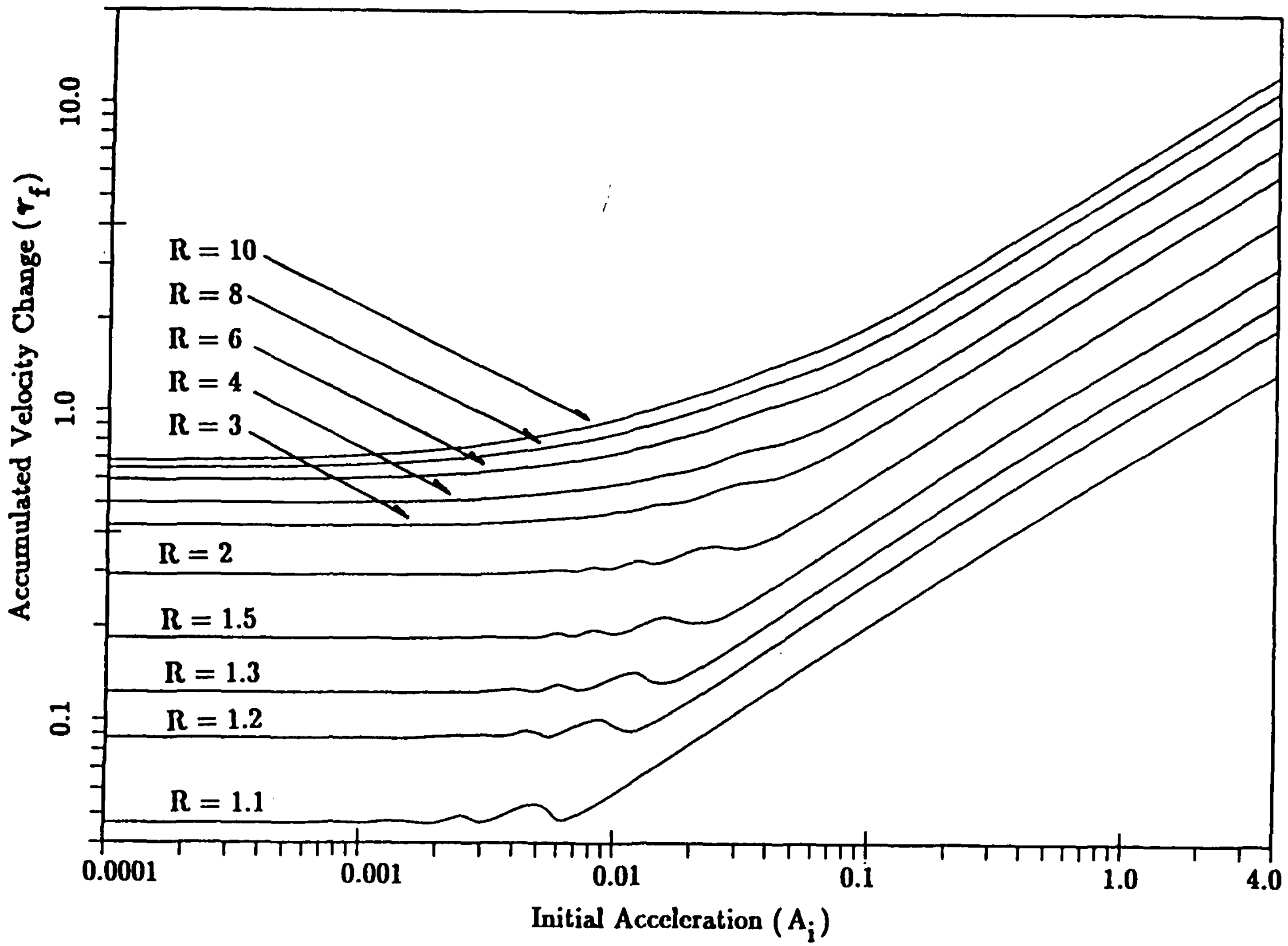

FIG. 2 Υ_f contours for various orbit ratios R ($m_p = 0.25$)

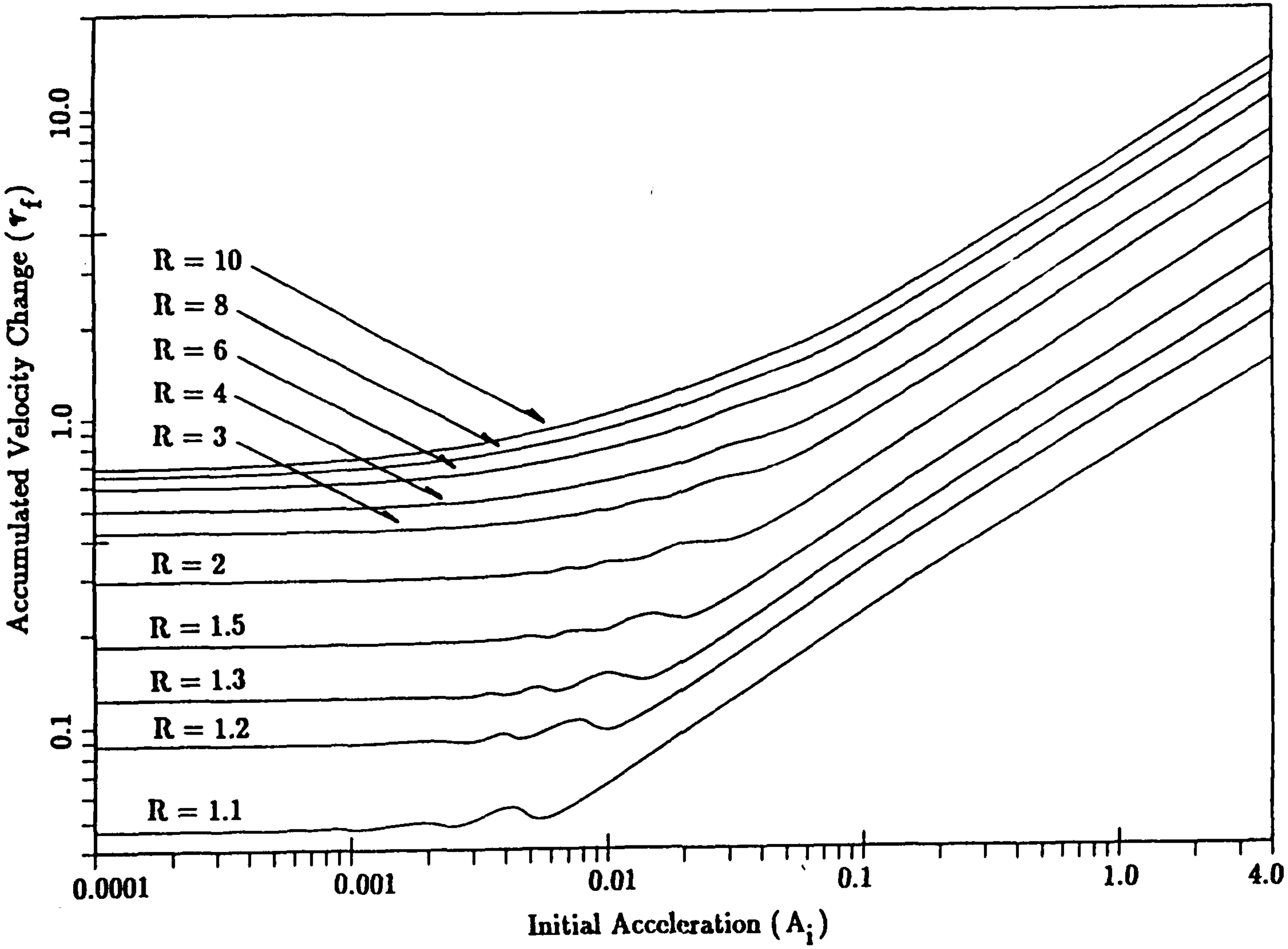

FIG. 3 γ_f contours for various orbit ratios R ($m_p = 0.5$)

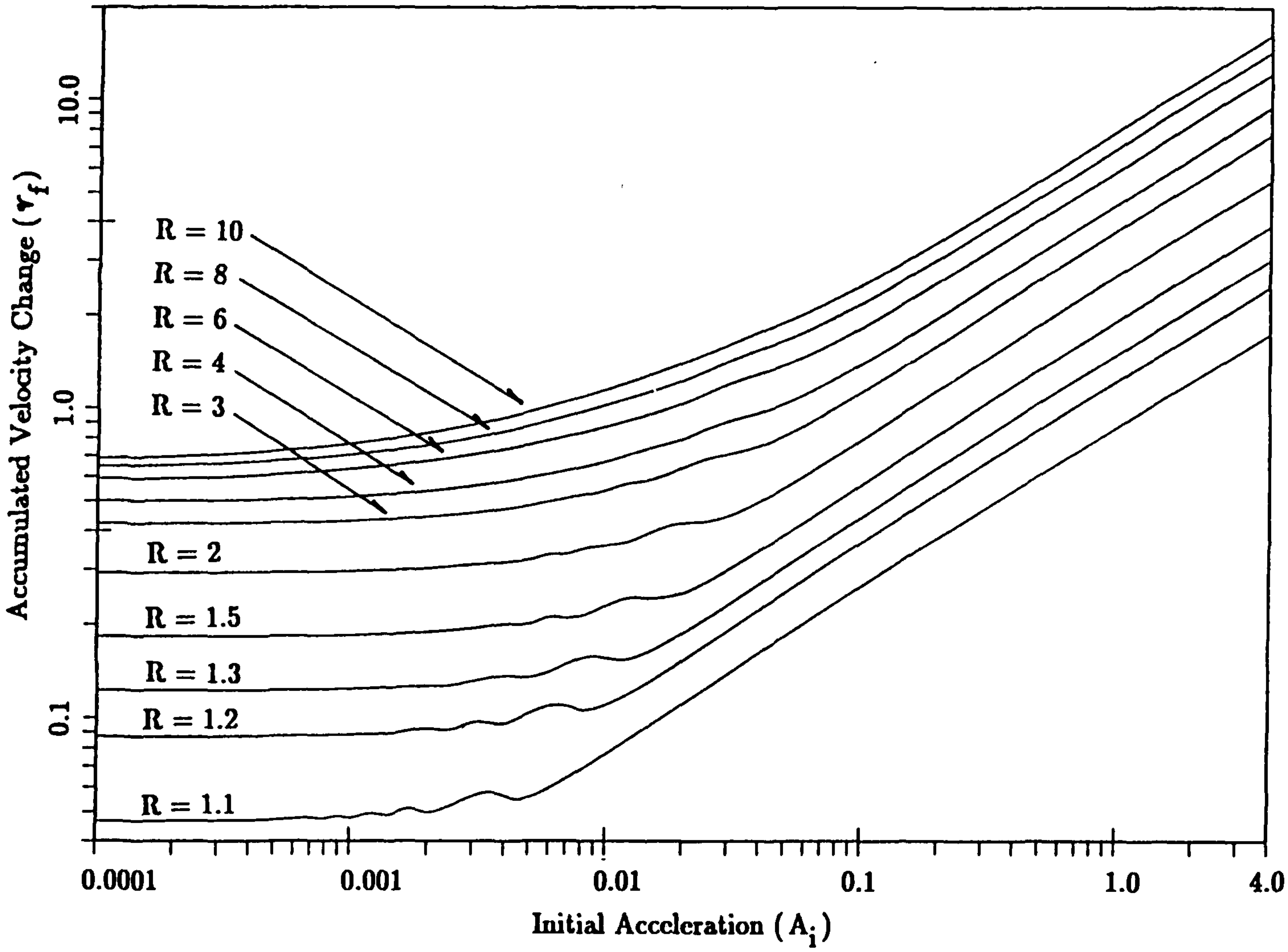

FIG. 4 Υ_f contours for various orbit ratios R ($m_p = 0.75$)

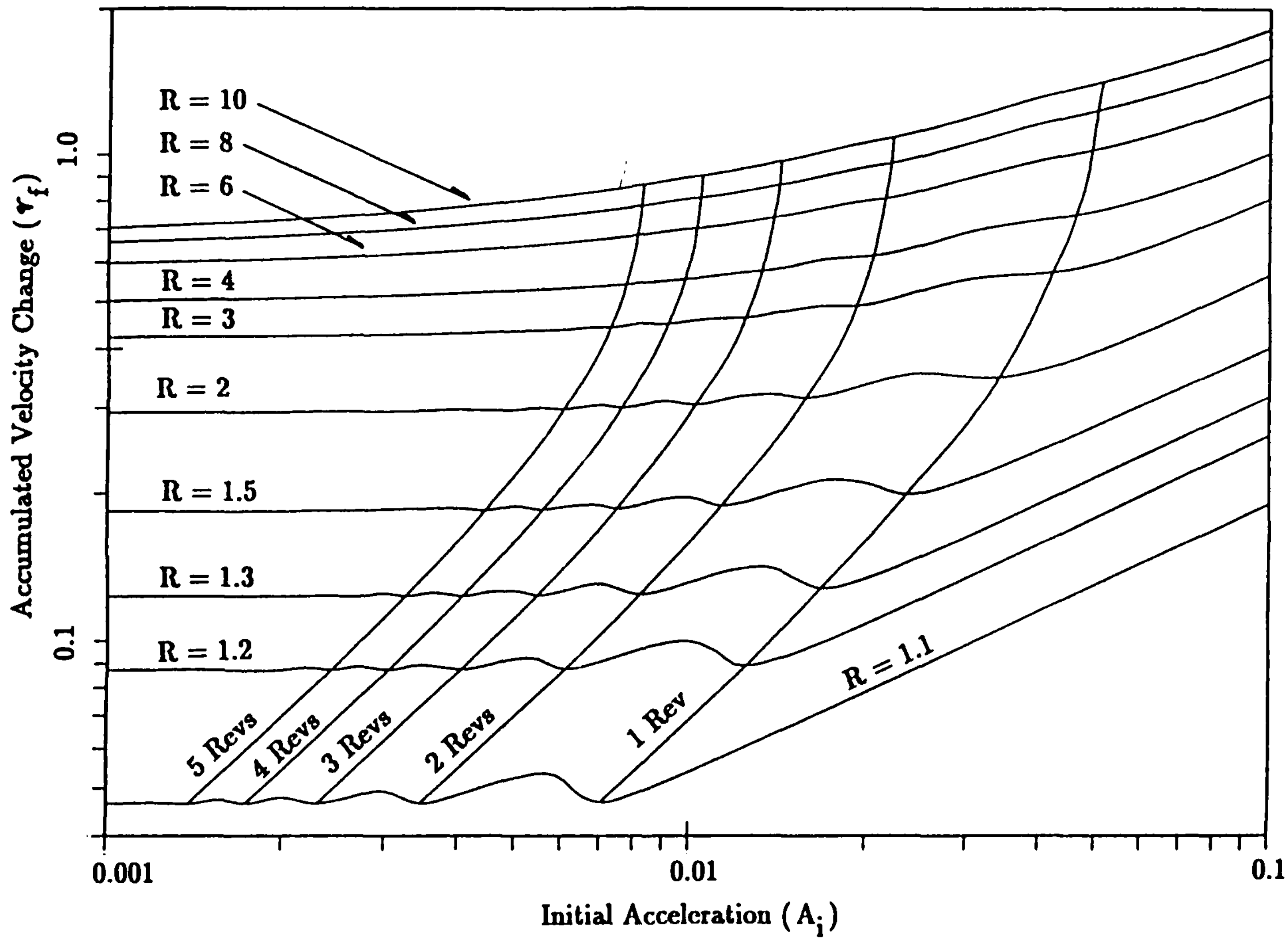

FIG. 5 Υ_f contours with superimposed revolution lines ($m_p = 0$)

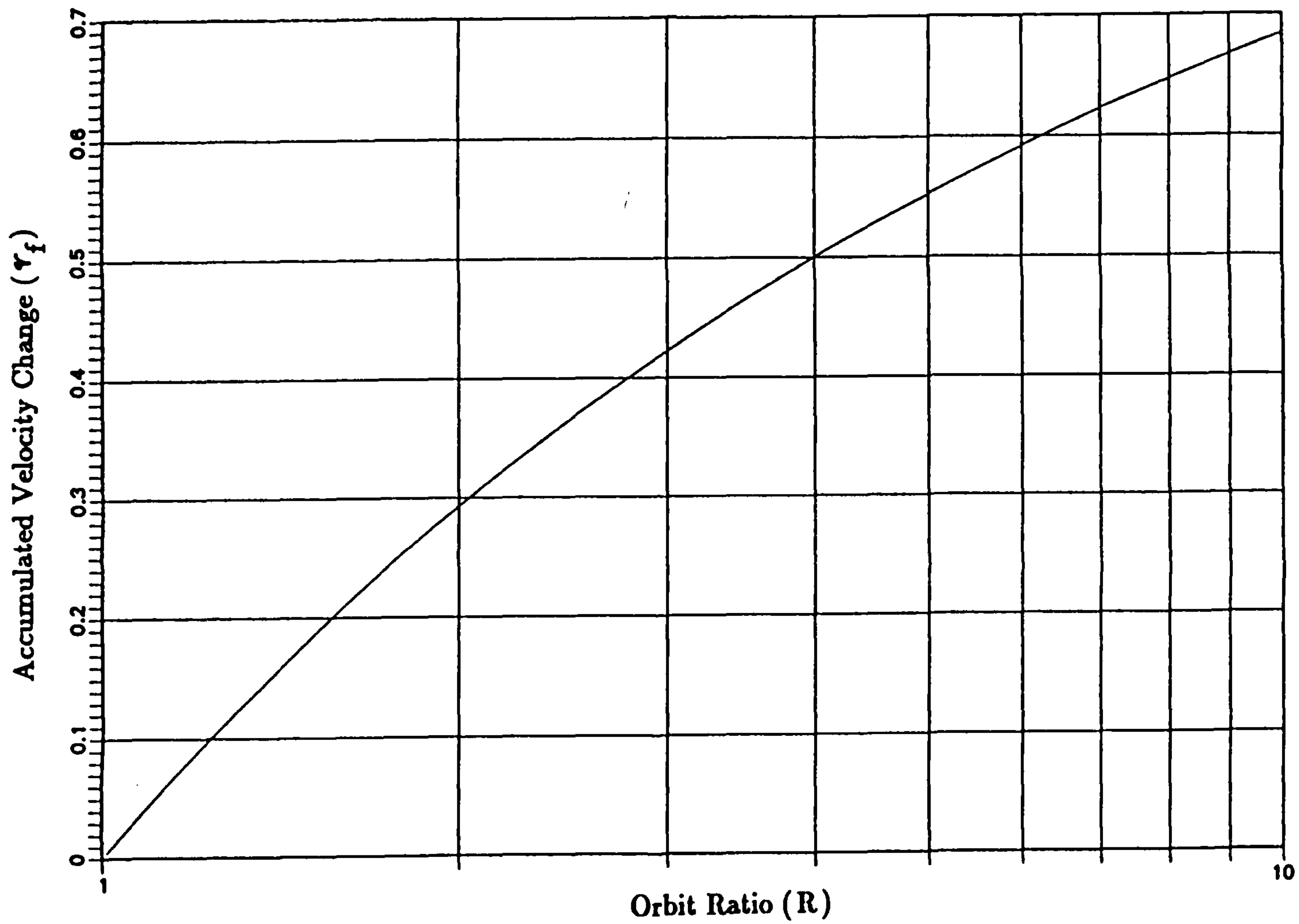

FIG. 6 Υ_f contour for low thrust ($A_i < 10^{-4}$)

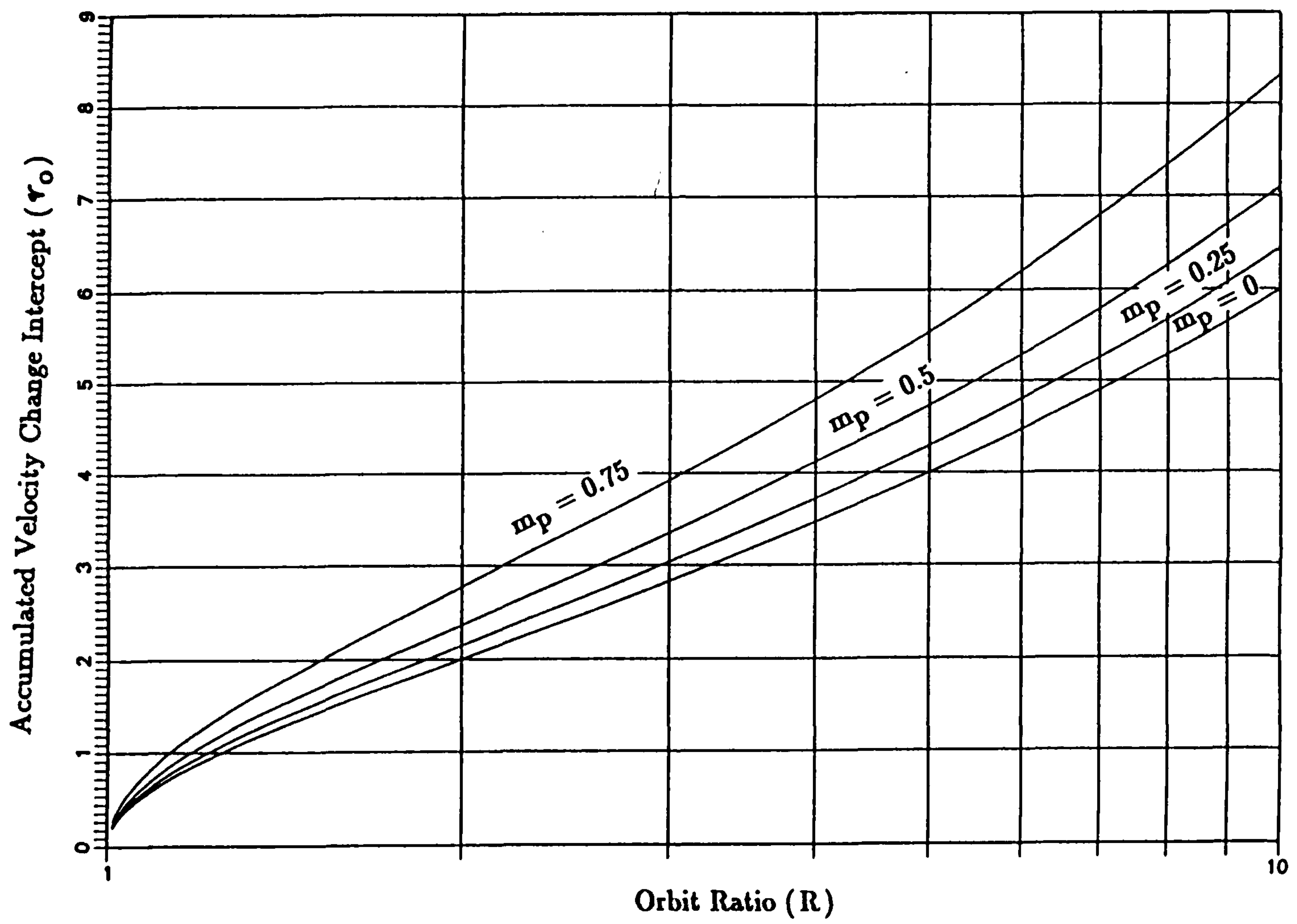

FIG. 7 Υ_o contours for high thrust ($A_i > 4$)